Nuclear Engineering and Design 317 (2017) 100–109

Contents lists available at ScienceDirect

Nuclear Engineering and Design

journal homepage: www.elsevier.com/locate/nucengdes

# Natural convection of the oxide pool in a three-layer configuration of core melts

Su-Hyeon Kim, Hae-Kyun Park, Bum-Jin Chung *

*Department of Nuclear Engineering, Kyung Hee University, 1732 Deogyeong-daero, Giheung-gu, Yongin-si, Gyeonggi-do 17104, Republic of Korea*

## HIGHLIGHTS

- Natural convection of oxide pool in 3-layer configuration during IVR was investigated.
- High Ra was achieved by using mass transfer experiments based on analogy concept.
- Heat ratio to light metal layer was 14% higher for 3-layer configuration than 2-layer one.
- Heat transfer to heavy metal layer was poor and hence heat load to side wall increased.
- Angular heat loads to side wall showed strengthened heat focusing at uppermost location.

## ARTICLE INFO

*Article history:*
Received 15 November 2016
Received in revised form 24 March 2017
Accepted 26 March 2017

*Keywords:*
In-Vessel Retention
Oxide pool
Three-layer configuration
Natural convection
Analogy
Mass transfer

## ABSTRACT

We investigated the natural convection of the oxide layer in a three-layer configuration of core melts in a severe accident. In order to achieve high modified Rayleigh numbers of $10^{12}$–$10^{13}$, mass transfer experiments were performed using a copper sulfate electroplating system based upon the analogy between heat and mass transfer. Four different cooling conditions of the top and the bottom plates were tested. The upward heat ratios were 14% higher for three-layer than for two-layer due to the reduced heights and the downward heat ratios were lower the same amount. The local Nusselt numbers for the top and the bottom plates were measured and compared with the two layer configuration. To explore the heat load to the reactor vessel, the angle-dependent heat fluxes at the side wall, were measured and compared with the two-layer configuration. Heat load to the side wall and peak heat at the uppermost location were intensified for the three-layer configuration.



## 1. Introduction

Fuels may melt and relocate to the lower vessel plenum in a severe accident, releasing the decay heat continuously. The IVR-ERVC (In-Vessel Retention-External Reactor Vessel Cooling) is an effective strategy for maintaining the reactor vessel integrity during a severe accident. The IVR strategy has been verified for small and medium sized plants such as AP600, AP1000 and Loviisa nuclear power plants, whose surface-to-volume ratios are large. Meanwhile, the EPR of 1800 MWe gave up the strategy and adopted the core catcher. The IVR strategy for APR-1400 are to be further verified whose power level is in between.

The molten fuels could be stratified into two-layer (upper light metal layer and lower oxide layer) or three-layer (upper light metal layer, middle oxide layer and lower heavy metal layer) by the density differences. Most studies have been performed for the two-layer configuration. Natural convective flows inside the oxide pool of two-layer and three-layer configurations are different due to the geometrical differences. Especially, the light metal layer of the three-layer configuration, becomes thinner than that of the two-layer system, resulting in the intensification of heat focusing to the reactor vessel. The oxide pool governs the entire heat transfer of the IVR as it supplies the decay heat to other metal layers with high heat conductivities. Thus, the phenomenological study is needed to explore the internal flow and heat transfer of the three-layer oxide pool, which imposes larger heat load to the reactor vessel. Especially, it is important to know the heat ratios of upward, side and downward.

We performed the natural convection experiments of the oxide layer in three-layer configuration. We employed the mass transfer experiments using a copper sulfate–sulfuric acid ($CuSO_4$–$H_2SO_4$) electroplating system based on the heat and mass transfer analogy concept. By performing mass transfer experiments, we could

* Corresponding author.
*E-mail address:* bjchung@khu.ac.kr (B.-J. Chung).

http://dx.doi.org/10.1016/j.nucengdes.2017.03.036
0029-5493/

**Nomenclature**

| | |
|---|---|
| $A$ | Area [$m^2$] |
| $C$ | Molar concentration [$kmole/m^3$] |
| $D_m$ | Mass diffusivity [$m^2/s$] |
| Da | Damköhler number ($q'''H^2/k\Delta T$) |
| $F$ | Faraday constant [96,485 *Coulomb/mole*] |
| $g$ | Gravitational acceleration [9.8 $m/s^2$] |
| $Gr_H$ | Grashof number ($g\beta\Delta TH^3/\nu^2$) |
| $h_h$ | Heat transfer coefficient [$W/m^2 K$] |
| $h_m$ | Mass transfer coefficient [$m/s$] |
| $H$ | Height [$m$] |
| $I$ | Current density [$A/m^2$] |
| $I'''$ | Current per volume [$A/m^3$] |
| $I_{lim}$ | Limiting current density [$A/m^2$] |
| $k$ | Thermal conductivity [$W/m K$] |
| $n$ | Number of electrons in charge transfer reaction |
| Nu | Nusselt number ($h_hH/k$) |
| Pr | Prandtl number ($\nu/\alpha$) |
| $Q$ | Heat quantity [$W$] |
| $q$ | Heat generation rate [$W$] |
| $q'''$ | Volumetric heat generation rate [$W/m^3$] |
| $R$ | Radius corresponding to pool [$m$] |
| $Ra_H$ | Rayleigh number ($Gr$Pr) |
| $Ra'_H$ | Modified Rayleigh number ($Ra_H$Da) |
| Sc | Schmidt number ($\nu/D_m$) |
| Sh | Sherwood number ($h_mH/D_m$) |
| $T$ | Temperature [$K$] |
| $t_{Cu}^{2+}$ | Transference number of $Cu^{2+}$ |
| $U_x$ | Uncertainty of $x$ |

*Greek symbols*

| | |
|---|---|
| $\alpha$ | Thermal diffusivity [$m^2/s$] |
| $\beta$ | Volume expansion coefficient [$1/K$] |
| $\gamma$ | Dispersion coefficient |
| $\mu$ | Viscosity [$kg/m\ s$] |
| $\nu$ | Kinematic viscosity [$m^2/s$] |
| $\rho$ | Density [$kg/m^3$] |

*Subscripts*

| | |
|---|---|
| *b* | Bulk |
| *bottom* | Bottom plate |
| *dn* | Downward |
| *h* | Heat transfer system |
| *m* | Mass transfer system |
| *side* | Side wall |
| *T* | Thermal |
| *up* | Upward |

achieve high buoyancies with small facilities. The test facility is semi-circular with chopped bottom, simulating the oxide pool above the heavy metal layer in a three-layer configuration (MassTER-OP2-HML: Mass Transfer Experimental Rig for a 2-D Oxide Pool above Heavy Metal Layer). The $Ra'_H$ ranged from $10^{12}$ to $10^{13}$. We measured the heats at the top plate, the side wall and the bottom plate, and compared these results with those for a two-layer configuration.

## 2. Theoretical background

### 2.1. Phenomena

In a severe accident, the molten core relocates to the lower vessel plenum. Generally, it is assumed that the metallic materials, such as Fe and Zr, and the oxidic materials, such as $UO_2$ and $ZrO_2$, are stratified into two-layer by the density difference, as shown in Fig. 1(a). However, MASCA experiment (Barrachin and Defoort, 2004) reported that when Zr is not oxidized sufficiently, the U migrates to the metal layer, increasing the density of metal layer. Then, it leads to the layer inversion and an additional heavy metal layer is formed at the bottom, resulting in three-layer configuration as shown in Fig. 1(b). The top layer contains Fe and Zr. The middle oxide layer consists of $UO_2$, $ZrO_2$ and most of the fission products. The bottom heavy metal layer contains U, Fe and Zr with some metallic fission products. The thickness of the light metal layer decreases due to the formation of heavy metal layer, which would then enhance the heat focusing to reactor vessel in the metal layer.

In a three-layer configuration, the geometry of oxide layer becomes the chopped hemi-sphere as shown in Fig. 2. The decay heat is transferred to the top plate, the side vessel and the bottom plate.

Fig. 3(a) indicates the flow patterns of oxide layer in two-layer configuration (Bonnet and Seiler, 1999). The external cooling forms the natural convective flows which run down along the curved surface and merge at the bottom. Then, these flows move upward and disperse towards the edge at the top plate. There are also natural convective flows underneath the top cooling plate. As there was no detailed explanation for three-layer configuration in the existing studies, we expect the three-layer flows are similar with the two-layer flows as shown in Fig. 3(b).

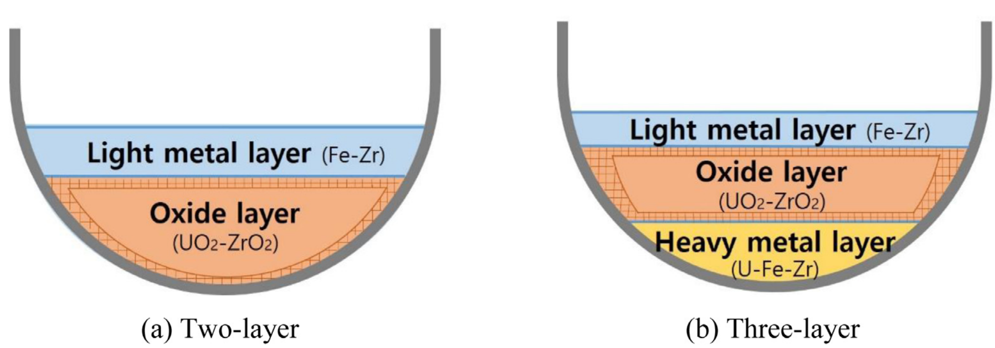


**Fig. 1.** Stratified molten pool configuration.